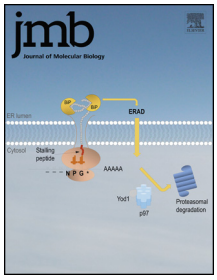

Regulation of Human Hsc70 ATPase and Chaperone Activities by Apg2: Role of the Acidic Subdomain

Yovana Cabrera [1], Leire Dublang [1], José Angel Fernández-Higuero [1], David Albesa-Jové [2,3], Maria Lucas [2,4], Ana Rosa Viguera [1], Marcelo E. Guerin [2,3], Jose M.G. Vilar [1,3], Arturo Muga [1] and Fernando Moro [1]

*1 - **Instituto Biofisika (UPV/EHU,** CSIC) y Dpto. de Bioquímica y Biología Molecular, Facultad de Ciencia y Tecnología, Universidad del País Vasco, Barrio Sarriena S/N, 48490, Leioa, Spain*
*2 - **Structural Biology Unit,** CIC bioGUNE, Bizkaia Technology Park, 48160 Derio, Spain*
*3 - **IKERBASQUE,** Basque Foundation for Science, 48013 Bilbao, Spain*
*4 - **IBBTEC,** C/ Albert Einstein 22, PCTCAN, 39011 Santander, Spain*

***Correspondence to Fernando Moro:** fernando.moro@ehu.es.*
https://doi.org/10.1016/j.jmb.2018.11.026
Edited by Judith Frydman

Abstract

Protein aggregate reactivation in metazoans is accomplished by the combined activity of Hsp70, Hsp40 and Hsp110 chaperones. Hsp110s support the refolding of aggregated polypeptides acting as specialized nucleotide exchange factors of Hsp70. We have studied how Apg2, one of the three human Hsp110s, regulates the activity of Hsc70 (HspA8), the constitutive Hsp70 in our cells. Apg2 shows a biphasic behavior: at low concentration, it stimulates the ATPase cycle of Hsc70, binding of the chaperone to protein aggregates and the refolding activity of the system, while it inhibits these three processes at high concentration. When the acidic subdomain of Apg2, a characteristic sequence present in the substrate binding domain of all Hsp110s, is deleted, the detrimental effects occur at lower concentration and are more pronounced, which concurs with an increase in the affinity of the Apg2 mutant for Hsc70. Our data support a mechanism in which Apg2 arrests the chaperone cycle through an interaction with Hsc70(ATP) that might lead to premature ATP dissociation before hydrolysis. In this line, the acidic subdomain might serve as a conformational switch to support dissociation of the Hsc70:Apg2 complex.

Introduction

Reactivation of protein aggregates is one of the most challenging tasks of the cellular proteostasis network. Aggregates might originate from stress situations, mutations or conformational transitions that destabilize the native conformation of a protein. Many human disorders are linked to protein aggregation processes, pointing out their potential toxicity. Cells are able to eliminate protein aggregates using different combinations of molecular chaperones (reviewed in Refs. [1–3]). In metazoans, the disaggregase activity relies on the cooperation of Hsp70, Hsp40 and Hsp110 chaperones [4–6], being the last one the less studied chaperone in this trio. Hsp110s are closely related to the Hsp70 family, sharing both sequence and structural homology [7]. These proteins are relatively abundant in mammalian and yeast cells, and their expression is regulated by different types of stress [8,9]. Among other proteins in the eukaryotic cytosol, as Bag1 and HspBP1, Hsp110s possess a strong nucleotide exchange activity on their Hsp70 counterparts [10,11]. Besides the nucleotide exchange factor (NEF) activity, several reports in the literature point out that human Hsp110 prevents protein aggregation, promotes folding and confers heat resistance to cells [12–14]. Furthermore, the biogenesis and quality control of several proteins related to human disorders, as CTFR and SOD1, depend on Hsp110 activity [15–17]. These studies suggest that Hsp110s act as chaperones able to remodel the conformation of their protein substrates, but the precise role of Hsp110 in protein disaggregation remains controversial [2,3].

Similarly to Hsp70s, chaperones of the Hsp110 family are built of two domains (Fig. 1a): an N-terminal nucleotide binding domain (NBD), able to bind and

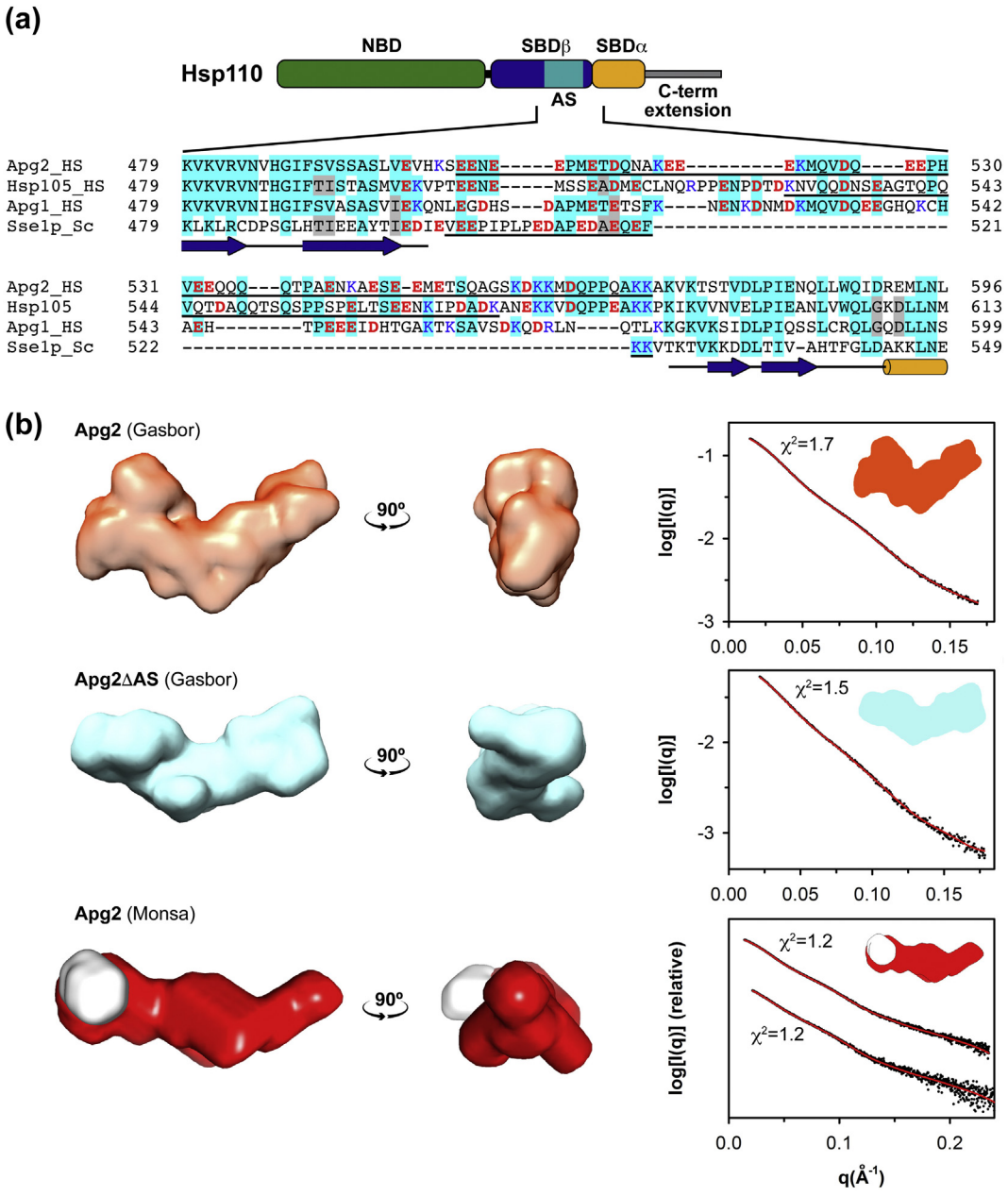

Fig. 1. Low-resolution models of Apg2 and Apg2ΔAS. a, Schematic representation of Apg2 structure and sequence alignment of the AS of human Apg2, Hsp105 and Apg1, and yeast Sse1p. Identical residues are highlighted in cyan. Underlined residues correspond to the sequence deleted in Apg2 (this work) and Sse1p [19] and the sequence missing in Hsp105β due to alternative splicing. Structural elements of Sse1p are shown. b, *Ab initio* envelope reconstructions of Apg2. SAXS data of Apg2 and Apg2ΔAS were used for envelope reconstructions using GASBOR and MONSA. For each predicted envelope, two views are shown related by a 90° rotation. The SAXS data and the corresponding fitting to the predicted envelope are shown on the right panel; the corresponding χ^2 value is also indicated.

hydrolyze ATP, and a C-terminal substrate binding domain (SBD) that contains a polypeptide binding site (Xu 2012), which can be divided into α and β subdomains (SBD-α and SBD-β). The SBD of Hsp110s harbors the main structural divergences with Hsp70s, consisting in (i) insertion of an acidic subdomain (AS) in the SBD-β and (ii) an intrinsically disordered C-terminal extension. These protein regions are present in both metazoan and yeast Hsp110, being significantly larger in the former [1]. The available structures of *Saccharomyces cerevisiae* Sse1p show that both the AS and the C-terminal domain are disordered [18,19]. The AS can be observed as a loop protruding from the SBD-β due to the order

induced by crystal packing [20]. The precise role of these domains on Hsp110 activity remains poorly understood. Both the AS and the C-terminal domain are involved in the correct cytoplasmatic and nuclear localization of isoforms α and β of Hsp105, respectively [21,22]. A construct lacking the last 19 residues from Sse1p C-terminal domain has impaired nucleotide exchange activity [10]. However, deletion of the last 44 unstructured residues does not abolish the ability to confer thermal resistance to yeast cells [23]. Elimination of the AS in human Hsp110 reduces the refolding activity of the protein, without significantly affecting its ability to prevent aggregation of a protein substrate [13]. In agreement with these data, a similar deletion in yeast Sse1p slightly decreases the refolding rate of a substrate held in a folding-competent conformation, without modifying its interaction with Ssa1p and the nucleotide exchange activity [19].

Here we investigate how Apg2 (HSPH2), one of the three representatives of the Hsp110 family in humans, regulates the Hsc70 system, by measuring its effect on chaperone binding to unfolded and aggregated substrates, and on the refolding and the ATPase activities of the complete disaggregase system. We found that these activities are stimulated by low Apg2 concentrations, while high amounts of the chaperone cause a strong inhibition. With the aim to study the specific role of the divergent AS, we used an Apg2 mutant lacking residues 504 to 569. The sequence of this protein region shows a low degree of conservation and is characterized by a high content of acidic amino acids and a central region enriched in Q/P residues (Fig. 1a). The resulting mutant, termed Apg2ΔAS, showed an increased affinity for Hsc70 that resulted in a premature inhibition of the ATPase and refolding activities of the chaperone system and a stronger ability to interfere with binding of Hsc70 to protein aggregates. Our data indicate that the AS might act as a conformational switch to allow optimal dissociation of Hsc70:Apg2 complexes.

Results

Structural analysis of Apg2 and Apg2ΔAS

In order to study the role of the AS in the activity of Apg2, we designed the deletion mutant Apg2ΔAS lacking residues 504 to 569 (Fig. 1a). First, small-angle X-ray scattering (SAXS) and circular dichroism spectra showed that deletion of the AS sequence did not significantly modify (i) the secondary structure content and (ii) overall fold of the protein (Fig. 1b; Supplementary Figs. S1A and S2A). Pairwise comparison of Apg2 and Apg2ΔAS scattering curves indicated a reasonable level of similarity (χ^2 = 2.6); which correlated well with estimated structural parameters, such as radius of gyration (R_g), maximum dimension (D_{max}), Porod volume and molecular weight (Supplementary Table 1). The *ab initio* reconstructions of Apg2 and Apg2ΔAS predicted elongated *V*-shaped envelopes. Interestingly, simultaneous fitting of Apg2 and Apg2ΔAS SAXS curves during multiphase bead modeling, as implemented in MONSA, permitted the *ab initio* location of the AS protruding from the reconstructed Apg2 envelope, suggesting that this subdomain might adopt a globular folded conformation (Fig. 1b). Furthermore, comparison between the calculated scattering curve of the yeast homolog Sse1p 3D structure (PDB code 3D2E) [19] and the experimental scattering curves of Apg2 or Apg2ΔAS indicated a high level of discrepancy (Apg2 *versus* Sse1p χ^2 = 186.49; Apg2-ΔAS *versus* Ses1p χ^2 = 27.0). This is not surprising, given that Apg2 is a larger protein compared to the Sse1p construct used to obtain the crystal structure (PDB code 3D2E), containing 46 and 135 more residues at the AS and C-terminal domains, respectively. In order to reconcile the crystal structure of the yeast homolog with the scattering curves of the Apg2 or Apg2ΔAS, we generated a structural model for the full-length protein combining homology modeling and *de novo* peptide structure prediction (see Materials and Methods for details). Comparison of the calculated scattering curves of final refined atomistic models with the corresponding experimental curves indicated a reasonable level of agreement (Supplementary Fig. S1B; χ^2 = 1.4 and 1.9 for Apg2ΔAS and Apg2 atomistic models, respectively). Similar to *ab initio* envelope reconstructions, the atomistic models suggest that Apg2 adopts and elongated *V*-shaped structure with the AS sequence forming a discrete domain projecting from the SBD. Finally, we compared the stability of Apg2 and Apg2ΔAS following the thermal denaturation of the proteins by circular dichroism. Apg2 displayed a cooperative denaturation profile, as found elsewhere [24], with a denaturation midpoint of 51.4 ± 0.6 °C (Supplementary Fig. S2B). As expected from the results shown above, the truncation mutant showed a main denaturation transition similar to the wt protein, emphasizing that deletion of the AS did not affect the global folding of the protein. Taking together, these data show that deletion of residues 504–569 did not significantly modify the folding pattern of the protein.

The AS is required for efficient refolding of unfolded and aggregated protein substrates

In order to test the chaperoning activity of the AS deletion mutant, we first studied the refolding of protein substrates protected from aggregation by Apg2 or Apg2ΔAS, as shown for different Hsp110 proteins [10,12,25,26]. Luciferase (0.1 μM) was denatured at 42 °C in the absence or presence of wt Apg2 or Apg2ΔAS at 0.4 μM and 2 μM, and refolding was initiated by addition of Hsc70 and DnaJB1 (2 and 1 μM, respectively). After incubation for 1 h at 30 °C,

approximately 50% of the luciferase activity was recovered when protection was carried out with 0.4 μM Apg2, increasing the yield up to 60% at 2 μM (Fig. 2a, middle panel). At both concentrations, Apg2 was very efficient avoiding aggregation of thermally denatured luciferase (Fig. 2b), in agreement with others [5]. A similar behavior was observed for the truncation mutant Apg2ΔAS, which was marginally less efficient at 0.4 μM. However, the amount of the substrate refolded by the complete disaggregase system was over 60% when Apg2ΔAS was used as holdase at this concentration (Fig. 2a, middle panel). Surprisingly, reactivation was reduced approximately to two thirds when the concentration of the mutant was raised to 2 μM, albeit protection from aggregation was similar to that found for wt Apg2 (Fig. 2b). These results demonstrate that deletion of the AS does not hamper the interaction of the mutant with unfolded substrates, avoiding their aggregation, but decreases the refolding efficiency by the complete human disaggregase system (Hsc70/DnaJB1/Apg2) in a concentration-dependent manner. When the thermal unfolding of luciferase was carried out in the absence of chaperones, the resulting aggregates were refolded with lower efficiency by the Hsc70/DnaJB1/Apg2 system (Fig. 2a, right panel), in agreement with published results [5]. Wt Apg2 could support the reactivation of only 30% of the initially aggregated luciferase regardless of the concentration used, whereas the refolding activity in the presence of Apg2ΔAS was concentration-dependent, being wt-like at low concentration (0.4 μM) and almost negligible at 2 μM (Fig. 2a, right panel).

Then, we studied the refolding of protein aggregates that are reactivated more efficiently by human Hsp70, Hsp40 and Hsp110 chaperones, as previously shown [5,14] (Fig. 2c). According to these studies, two different substrates were used: luciferase aggregates formed after denaturation in 8 M urea and removal of the chaotropic agent by dilution, and glucose 6-phosphate dehydrogenase (G6PDH) aggregates obtained after thermal denaturation at 50 °C for 10 min. In both cases, refolding experiments

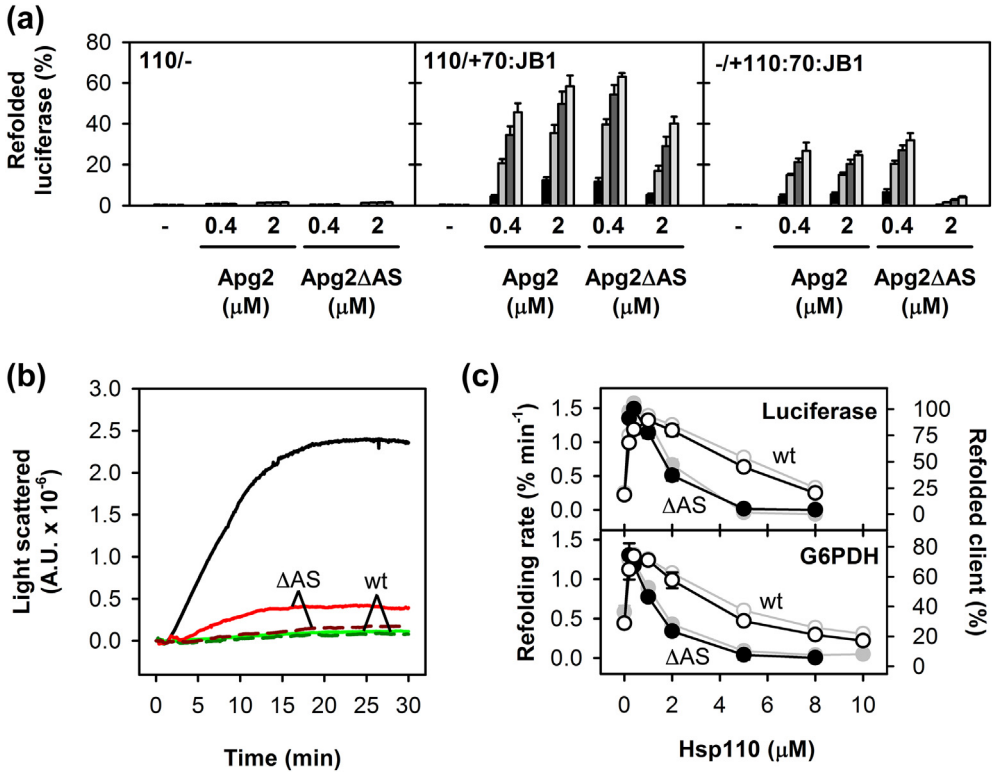

Fig. 2. The AS is required for efficient refolding of unfolded and aggregated protein substrates. a, Luciferase (0.1 μM) was denatured for 30 min at 42 °C in the presence of wt Apg2 or Apg2ΔAS at 0.4 and 2 μM (left and middle panels). Refolding was initiated at 30 °C by no further addition (left panel) or addition of 2 μM Hsc70 and 1 μM DnaJB1 (middle panel). (Right panel) Luciferase (0.1 μM) was denatured for 30 min at 42 °C in the absence of chaperones and refolding was performed by addition of 2 μM Hsc70, 1 μM DnaJB1, 0.4 or 2 μM wt Apg2/Apg2ΔAS, as indicated. Aliquots were taken at 10, 20, 40 and 60 min to analyze luciferase activity (black and gray bars). b, Aggregation of luciferase (0.1 μM) at 42 °C followed by light scattering at 320 nm in the absence of chaperones (black line) or in the presence of wt Apg2 (green lines) or Apg2ΔAS (red lines) at 0.4 (continuous lines) and 2 μM (dashed lines). c, Refolding of luciferase and G6PDH aggregates was performed in the presence of 2 μM Hsc70, 1 μM DnaJB1 and increasing concentrations of wt Apg2 (open circles) or Apg2ΔAS (closed circles). Refolding rates (black symbols) and yields after incubation for 2 h with the chaperones (gray symbols) are shown.

were carried out at fixed concentrations of Hsc70 and DnaJB1 (2 and 1 μM, respectively), and increasing amounts of wt Apg2 and Apg2ΔAS. At low concentration, addition of Apg2 or Apg2ΔAS similarly enhanced the refolding rate and yield of luciferase and G6PDH aggregates by Hsc70 and DnaJB1 (Fig. 2c). As previously found [5,27], increasing the concentration of Apg2 had a detrimental consequence in the refolding reaction and a steady decrease of the rate and yield was observed. In contrast to the wt protein, the reactivation activity decayed more rapidly as the concentration of Apg2ΔAS was raised. The strongest difference between the two protein variants was observed at 2 μM where the refolding rate for Apg2ΔAS was almost similar to that observed for Hsc70/DnaJB1 in the absence of Hsp110. At this mutant concentration, the reactivation rate and yield were reduced 3-fold, a stronger effect compared to the 1.5-fold reduction observed when luciferase was unfolded but held in a folding competent conformation by the chaperone (Fig. 2a, middle panel). Higher protein concentrations progressively diminished the difference between the wt and the truncation mutant, which inhibited the refolding reaction below the level observed for Hsc70/DnaJB1 alone. These results show that the AS is involved in the regulation of the chaperone activity of the human Hsc70/DnaJB1/Apg2 system, but it is important to note that the effect of the deletion of this subdomain is only evident when cochaperone concentration is unbalanced. The conformational properties of the substrate also seem to be crucial, as the remodeling defect due to AS deletion is gradually increased from unfolded substrates to mild and stable aggregates.

Interaction of Hsc70 with protein aggregates is regulated by Apg2

Since aggregate reactivation requires the initial binding of the chaperones to the aggregate surface, where extraction of the polypeptide chains for their subsequent refolding takes place, we studied how isolated Hsc70, DnaJB1 and Apg2 and different combinations of the three chaperones interacted with G6PDH aggregates (Fig. 3a). We found that association of human Hsc70 to the aggregates followed a pattern similar to that found for bacterial DnaK [28], as the amount of Hsc70 bound to the substrate increased 5 times in the presence of DnaJB1 (Fig. 3c). Isolated DnaJB1 interacted slightly better than Hsc70 with the aggregate but the amount of aggregate-bound cochaperone did not change in the presence of Hsc70 and/or Apg2. Compared to Hsc70 and DnaJB1, Apg2 bound very poorly to the aggregate, and addition of DnaJB1 did not modify this interaction. Apg2 did not change Hsc70 recruitment to the aggregate, but interestingly, it doubled the amount of Hsc70 that cosedimented with the aggregate when combined with DnaJB1. This increase in the amount of aggregate-bound Hsc70 induced by Apg2 correlates very well with the observed initial stimulation of the refolding rate and yield by the NEF (Fig. 2c). In order to test if tightly bound ADP copurifying with Hsc70 (approximately 0.2–0.3 mol ADP/mol protein in our protein preparations) affected its interaction with the aggregate, nucleotide-free Hsc70 was produced using the protocol published by Gao *et al*. [29]. We observed the same amount of Hsc70 cosedimented with the aggregate using the original Hsc70 sample or nucleotide-free Hsc70 (Fig. 3c, inset), discarding any effect of ADP contamination.

Next, we studied the effect of Apg2 and Apg2ΔAS on the interaction of Hsc70 with G6PDH aggregates (Fig. 3b). At low concentration (0.4 μM), Apg2 and Apg2ΔAS increased the amount of Hsc70 associated with the aggregate, the wt protein being slightly more effective than the mutant form. Under these conditions, approximately 40% and 30% of the initially added Hsc70 (2 μM) was bound to the aggregate for Apg2 and Apg2ΔAS, respectively. A further increase in Hsp110 concentration progressively decreased the amount of aggregate-bound Hsc70, more markedly for Apg2ΔAS. Above 5 μM, the truncation mutant almost completely prevented binding of Hsc70 molecules to the aggregate surface. Apg2 and Apg2ΔAS, interacted similarly with aggregates, the amount of protein bound increasing linearly with the concentration (Fig. 3d). This indicates that deletion of the AS did not modify the interaction of Apg2 with protein aggregates, as found above for unfolded substrates. The fraction of Apg2 bound to the aggregate was constant throughout the titration (around 2% of total Apg2) and significantly smaller than that of Hsc70 in the concentration range studied, suggesting that Apg2 interacts with lower affinity with protein aggregates. In summary, these data show that DnaJB1 and Apg2 regulate binding of Hsc70 to G6PDH aggregates, and that the amount of chaperone recruited at the aggregate surface correlates well with the substrate reactivation activity (Fig. 2c).

Apg2 and, more prominently, Apg2ΔAS decelerate peptide release from Hsc70

In order to investigate whether Apg2 modifies the substrate binding properties of Hsc70, we have studied the association and dissociation of the peptide FYQLALT, known to bind with high affinity to Hsc70 [30]. Stable complexes of Hsc70 with Apg2 or Apg2ΔAS were formed by overnight incubation of equimolar amounts of both proteins in the presence of 50 μM ATP, conditions similar to those used by others to form stoichiometric Hsp70:Hsp110 complexes [31]. The presence of free Hsc70 was negligible when complexes were made at 2, 4, 6 and 8 μM as shown by size exclusion chromatography (Supplemental Fig. S3A). Then, we measured the binding kinetics of t-FYQLALT, the peptide labeled with 5-TAMRA at the N-terminus, to the complexes and free Hsc70. Binding curves were fitted to single exponentials to obtain the

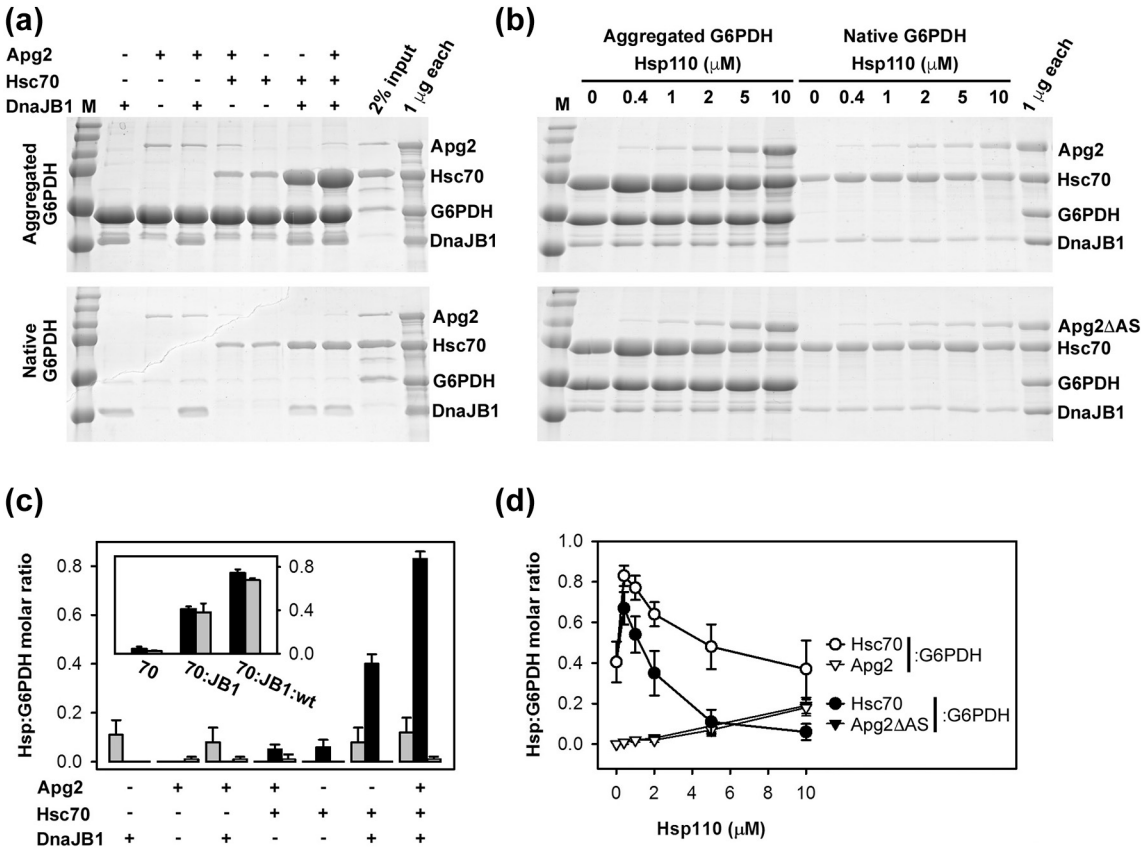

Fig. 3. Apg2 regulates the interaction of Hsc70 with protein aggregates. a, Interaction of Apg2 (0.4 μM), Hsc70 (2 μM) and DnaJB1 (0.5 μM) and different combinations of the chaperones as indicated with preformed G6PDH aggregates (upper panel). As a control, similar experiments were performed omitting the aggregation step (lower panel). Two percent of input proteins or 1 μg of each protein was loaded as reference. b, Binding of human chaperones to G6PDH as in panel a at increasing concentrations of Apg2 (upper panel) or Apg2ΔAS (lower panel). c, Quantification of DnaJB1 (gray bars), Hsc70 (black bars) and Apg2 (white bars) bound to the aggregate in panel a, expressed as molar ratio of G6PDH. (Inset) Cosedimentation of Hsc70 with the aggregate using the original Hsc70 preparation (black bars) or nucleotide-free Hsc70 (gray bars). d, Quantification of Hsc70 (circles) and Hsp110 (triangles) associated with aggregates expressed as molar ratio of G6PDH in the titrations in panel b of Apg2 (open symbols) and Apg2ΔAS (close symbols).

observed binding constant (K_{obs}). The on- and off-rate constants were obtained from the slope and *y*-intercept of the linear plot of K_{obs} *versus* complex concentration (Table 1 and Supplemental Fig. S3C). Our results indicate that the peptide binds with similar kinetics and affinity to Hsc70 either free or in complex with Apg2 orApg2ΔAS, excluding any effect of Apg2 on substrate binding to Hsc70.

Next, we measured the release of the substrate from Hsc70 induced by ATP and Apg2 or Apg2ΔAS (Fig. 4). Complexes between Hsc70 (1 μM) and t-FYQLALT (0.5 μM) were obtained by incubation in the presence of purified ADP, and dissociation was induced by addition of ATP alone or combined with increasing concentrations of Apg2 or Apg2ΔAS (Fig. 4a). Since nucleotide exchange is rate limiting, an increase of the dissociation constant is expected with increasing NEF concentrations. In contrast, the dissociation kinetics followed a biphasic behavior where both Hsp110 variants progressively and similarly accelerated peptide release up to 0.1 μM, while they slowed down the release kinetics above this concentration, the effect being stronger for Apg2ΔAS (Fig. 4b). Apg2 and the deletion mutant also reduced the amount of peptide released in the presence of ATP at high NEF concentration after equilibrium was reached, as seen by the higher final anisotropy values obtained in our experiments at 2 μM Apg2 and Apg2ΔAS (Fig. 4a). These results indicate that Apg2 and the deletion mutant induce a second process,

Table 1. Kinetic constants for binding of FYQLALT to Hsc70 and its complex with Apg2 or Apg2ΔAS

	k_{off} ($s^{-1} \times 10^{-3}$)	k_{on} (M^{-1} s^{-1})	K_D (μM)
Hsc70	0.32 ± 0.04	173 ± 11	1.8
Hsc70:Apg2	0.25 ± 0.07	165 ± 21	1.5
Hsc70:Apg2ΔAS	0.32 ± 0.004	160 ± 7	2

Values are the averages of two independent experiments. K_D was obtained from the k_{off}/k_{on} ratio.

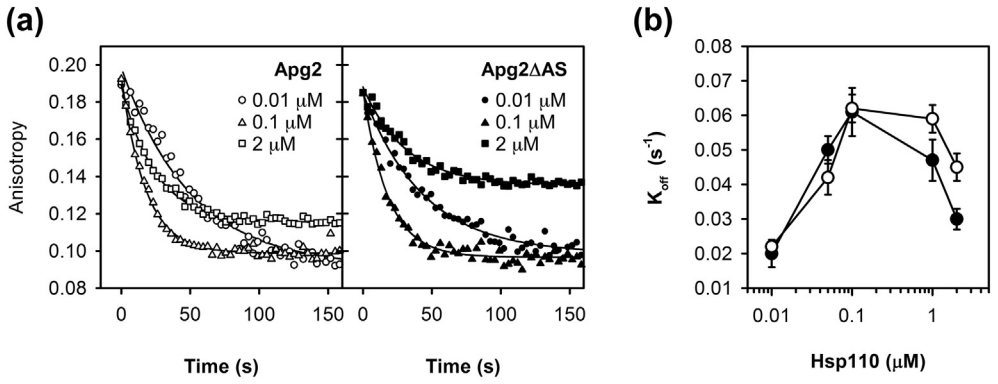

Fig. 4. Substrate dissociation from Hsc70 after ATP binding at increasing Apg2 and Apg2ΔAS concentrations. (a) Dissociation kinetics of preformed Hsc70(ADP):t-FYQLALT complexes after addition of 0.2 mM ATP and 0.01, 0.1 and 2 μM Apg2 (left) or Apg2ΔAS (right). Solid lines represent the best fits to a single exponential decay curve. (b) Observed K_{off} at increasing concentrations of Apg2 (open circles) or Apg2ΔAS (closed circles). K_{off} values are the average of three independent experiments.

besides nucleotide dissociation, that negatively impacts the substrate release kinetics and most likely involves peptide reassociation.

The AS modulates the ATPase stimulation of the Hsc70 system

To understand the functional defects that deletion of the AS caused in the Hsc70/DnaJB1/Apg2 system, the ATPase activity of the chaperone mixture was measured at increasing concentrations of Apg2 or Apg2ΔAS (Fig. 5). We first found that the truncation did not significantly modify the intrinsic ATPase activity of Apg2 as the steady-state activity varied from 0.74 ± 0.25 molATP molApg2^{-1} min^{-1} for the wt protein to 0.63 ± 0.18 for Apg2ΔAS (average values and standard deviations obtained from at least 10 different protein preparations). Then, we measured the ATPase activity of Hsc70 at increasing concentrations of the wt and mutant NEF in the absence and presence of DnaJB1 (Fig. 5a). In order to better observe the ATPase increment due to stimulation of the chaperone system, the concentration-dependent, linear increase of the basal activity of both proteins was subtracted from the experimental value. Wt Apg2 initially promoted a hyperbolic increase of the ATPase activity of the chaperone system reaching an apparent saturation at 3 μM, which turned out into a gradual inhibition above this concentration, in good agreement with previous observations with the human homolog Hsp105 [27,32]. Apg2ΔAS presented a stronger concentration-dependent biphasic behavior: at concentrations lower than 0.2–0.3 μM, it stimulated the ATPase activity of the chaperone system similarly to the wt protein, whereas above this point, a potent inhibitory effect was observed, reaching at 10 μM an activity value similar to that found in the absence of DnaJB1 (Fig. 5a). ATPase inhibition was not observed in the absence of DnaJB1, instead Apg2 and, with lower efficiency, Apg2ΔAS slightly stimulated Hsc70 within the concentration range studied. Next, we investigated whether deletion of the AS would hamper the nucleotide exchange activity of the protein in a concentration-dependent manner. Release of the fluorescent ADP analog MABA-ADP bound to Hsc70 was tested in the presence of increasing concentrations of Apg2 and Apg2ΔAS in a stopped-flow device (Fig. 5b). The observed dissociation rate constants followed a hyperbolic dependence with Apg2 concentration as found for Sse1p and other unrelated eukaryotic and prokaryotic NEFs as Fes1p and GrpE [10,33]. This indicates that acceleration of nucleotide release by Apg2 occurs through a two-step binding mechanism [33]. These measurements revealed that the nucleotide exchange activities of wt Apg2 and Apg2ΔAS were similar, in agreement with results obtained with a similar deletion mutant of Sse1p [19].

To quantify the dependence of the Hsc70 ATPase activity on the concentration of Apg2, we fitted the data to a concentration-dependent phenomenological model. Explicitly, we considered that Apg2 can affect both positively and negatively the ATPase cycle. Positive effects are expected from the NEF activity of Apg2 that promotes the release of ADP from Hsc70. We consider that this step happens at a rate $R = R_0 + C_R$[Apg2], where R_0 is the rate in the absence of Apg2 and C_R indicates how Apg2 concentration enhances ATP hydrolysis. Negative effects are modeled considering that the presence of Apg2 delays the completion of the ATPase cycle, which happens with a characteristic time given by $T = T_0 + C_T$[Apg2]. Here, T_0 is the time in the absence of Apg2 and C_T indicates how Apg2 concentration increases T. Taking into account both contributions, the ATPase activity for a given concentration [Hsc70] of Hsc70 is expressed as follows:

$$A_{\mathrm{ATPase}} = \frac{[\mathrm{Hsc70}]}{\frac{1}{R} + T} \qquad (1)$$

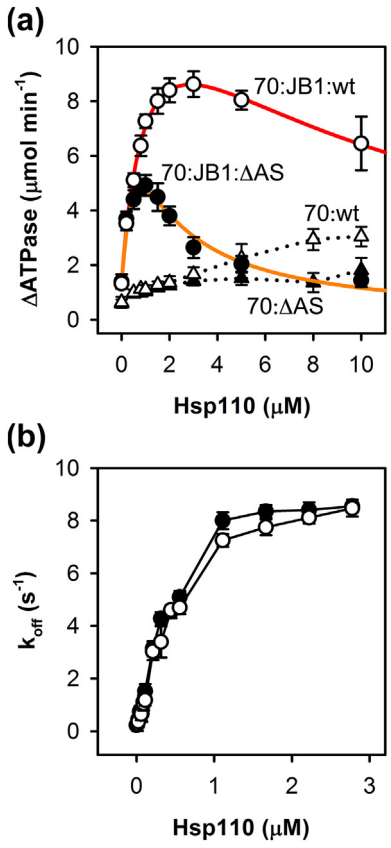

Fig. 5. Apg2 and Apg2ΔAS inhibit the ATPase activity of the Hsc70 system at high concentrations. (a) ATPase activity of 2 μM Hsc70 in the absence (triangles) and presence of 0.5 μM DnaJB1 (circles) was measured at increasing concentrations of wt Apg2 (open symbols) or Apg2ΔAS (closed symbols). ΔATPase values were obtained after subtraction of wt Apg2 and Apg2ΔAS basal activities. The red and orange lines represent the best fit to the phenomenological model [Eq. (1)] for wt Apg2 and Apg2ΔAS, respectively. The common values of the parameters of the model are R_0 = 0.766 min^{-1}, C_R = 7.15 μM^{-1} min^{-1}, and T_0 = 0.140 min. The value of C_T is 0.156 μM^{-1} min for Apg2ΔAS and 0.0158 μM^{-1} min for wt Apg2. (b) Nucleotide exchange activity of Apg2 (white symbols) and Apg2ΔAS (black symbols). Dissociation rates of MABA-ADP from Hsc70 were measured at increasing concentrations of Hsp110 proteins.

The model accurately captures the experimental measurements with values of R_0, C_R, and T_0 that are identical for both wt Apg2 and Apg2ΔAS (Fig. 5a). This result is consistent with the fact that there are no significant differences between the nucleotide exchange activities of wt Apg2 and Apg2ΔAS. The differences in the ATPase activity for the two types of Apg2 come from the C_T value, which is about 10 times higher for Apg2ΔAS.

Titrations were also performed at different DnaJB1 concentrations to determine the effect of the Hsp40 cochaperone on the ATPase activity of Hsc70 in the presence of Apg2 or App2ΔAS. Increasing DnaJB1 concentrations stimulated Hsc70 activity, reaching saturation at any Apg2 or Apg2ΔAS concentration tested (Supplementary Fig. S3). The inhibitory effect was evident for the truncated Hsp110 variant, as the saturation value reached in the stimulation curves by DnaJB1 increased until 1 μM Apg2ΔAS, and strongly decreased at higher protein concentrations (Supplementary Fig. S3B). A plot of the Apg2ΔAS concentration required to observe 50% reduction of the maximal ΔATPase as a function of DnaJB1 concentration showed a linear dependence (Fig. 6a). Thus, more Apg2ΔAS is required to inhibit the activity of the system at higher DnaJB1 concentrations, meaning that DnaJB1 rescues the inhibitory effect of the AS deletion mutant. This counteracting effect of DnaJB1 was also studied following the reactivation of luciferase and G6PDH aggregates. Experiments were performed at two concentrations of Apg2 and Apg2ΔAS: 0.4 μM, where both proteins behaved similarly, and 2 μM, an inhibitory concentration for Apg2ΔAS (Fig. 2c). As found for the bacterial DnaK system [34,35], increasing DnaJB1 concentrations reduced the refolding ability of Hsc70 in the presence of 0.4 and 2 μM Apg2, an effect that is better observed with G6PDH aggregates (Fig. 6b). A similar decrease of the refolding activity was found in the presence of 0.4 μM deletion mutant, while the inhibition induced by 2 μM Apg2ΔAS was partially and progressively compensated by DnaJB1 up to 5 μM. The inhibition of the refolding reaction was more prominent in the absence of Apg2, reflecting the compensatory effect of both cochaperones on the activity of the system. Taken together, these results suggest that the inhibition of the ATPase and refolding activities of the Hsc70 chaperone system observed at high Apg2 concentration results from an unbalanced DnaJB1:Apg2 molar ratio, which possibly impairs the productive timing of the Hsc70 ATPase cycle. They might also indicate a possible competition between Apg2 and DnaJB1 for Hsc70 binding.

The AS regulates the affinity of Apg2 for Hsc70

To gain further insight into the stronger inhibitory effect exerted by the AS deletion mutant, we contrasted the aforementioned phenomenological model with assays in which wt Apg2 and Apg2ΔAS competed for Hsc70 binding. First, the ATPase activity of Hsc70 (2 μM) in the presence of DnaJB1 (0.5 μM) and wt Apg2 (3 μM) was measured at increasing concentrations of the AS truncation mutant (Fig. 7a). Addition of Apg2ΔAS progressively reduced the ATPase activity, which reached values similar to those found in the absence of wt Apg2 (gray symbols). The inverse titration experiment in which increasing amounts of wt Apg2 were added to Hsc70 (2 μM) in the presence of DnaJB1 (0.5 μM) and Apg2ΔAS (3 μM), showed that, in contrast to the mutant, the wt protein could not restore the ATPase activity in the concentration range studied (Fig. 7b). These results indicate that the truncated

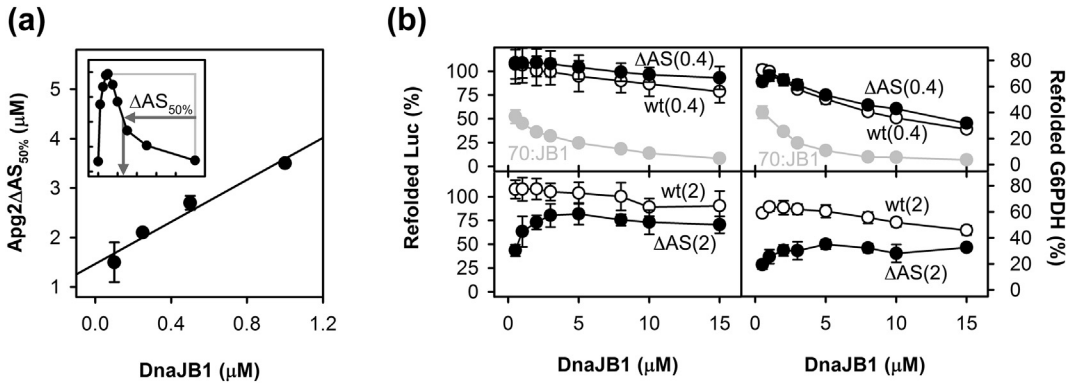

Fig. 6. DnaJB1 counteracts the inhibition of the ATPase and refolding activities induced by Apg2ΔAS. (a) Concentration of Apg2ΔAS at which 50% of the maximal activity of the Hsc70 system at different DnaJB1 concentrations is observed. (Inset) Schematic representation showing how $Apg2\Delta AS_{50\%}$ values were obtained at a given DnaJB1 concentration. (b) Refolding of luciferase and G6PDH aggregates after 2-h incubation with 2 μM Hsc70, 0.4 μM (upper panels) or 2 μM (lower panels) wt Apg2 (open circles) or Apg2ΔAS (closed circles) and increasing concentrations of DnaJB1. Gray symbols in upper panels represent the refolding yields in the absence of Apg2.

variant displaces wt Apg2 from Hsc70, exerting its stronger inhibitory effect. These experimental results could be precisely reproduced by the model using parameters inferred from titrations of wt Apg2 and Apg2ΔAS alone (Fig. 7, gray lines), and considering additive effects in the terms of Eq. (1). Explicitly, we use $R = R_0 + C_R([Apg2^{wt}] + [Apg2^{\Delta AS}])$ and $T = T_0 + C_T^{wt}[Apg2^{wt}] + C_T^{\Delta AS}[Apg2^{\Delta AS}]$ in Eq. (1), where the superscripts wt and ΔAS indicate the values of C_T and [Apg2] for wt Apg2 and Apg2ΔAS, respectively. Therefore, our model confirms that the positive effects of both proteins in the ATPase activity are the same and depend on just the sum of their concentrations, and that the negative effects are additive as well but with different strengths. These results are consistent with both proteins using similar mechanisms to activate/inhibit Hsc70, but with the ΔAS mutation leading to a 10-fold more potent arrest of the ATPase cycle, which might arise from an altered interaction with Hsc70.

This different behavior was further studied in the second type of experiments, in which formation of Hsc70:Hsp110 complexes in the absence of DnaJB1 was followed by native electrophoresis and surface plasmon resonance (SPR). It should be noted that Hsc70 and Apg2 run in native gels with a molecular size higher than their monomeric molecular weight calculated from the sequence (Fig. 6a). This is specially aggravated for the mutant Apg2ΔAS, which showed a much lower mobility. Similar deviations from the expected molecular weight were also observed by size exclusion chromatography; however, Apg2ΔAS eluted close to the wt protein, indicating that it has a similar size (Supplementary Fig. S5A). The lower electrophoretical mobility of Apg2ΔAS is possibly due to the deletion of a large clustered patch of negative charges. Despite the different mobility of the isolated proteins, the complexes of both wt Apg2 and Apg2ΔAS with Hsc70 showed apparent molecular weights more consistent with their theoretical values (Fig. 8a). Preformed Hsc70:Apg2 or Hsc70:Apg2ΔAS complexes were titrated with increasing concentrations of Apg2ΔAS or wt Apg2, respectively (Supplementary Fig. S5B). Quantification of the corresponding bands demonstrated that higher concentrations of wt Apg2 were required to displace Apg2ΔAS from the complex, as compared with the experiment in which wt Apg2 was easily displaced by Apg2ΔAS (Fig. 8b). Therefore, Apg2ΔAS competed efficiently with the wt protein to bind Hsc70, indicating that it binds to the chaperone with higher affinity.

In order to determine the equilibrium binding constants for the complexes of Hsc70 with wt Apg2 and Apg2ΔAS, SPR experiments were performed using a Hsc70 modified with a C-terminal streptag immobilized on a CM5 chip coated with anti-streptag antibody (Fig. 8c). Injection of Apg2 or Apg2ΔAS in the absence of nucleotides resulted in sensograms with fast association and dissociation kinetics (Supplementary Fig. S5C), in agreement with previous observations with yeast Sse1p [36]. As Raviol and coworkers [36] found, inclusion of ATP did not allow binding of Apg2 or Apg2ΔAS to Hsc70 in our SPR setup. When purified ADP was used, we found a strong affinity reduction of at least 2 orders of magnitude (Fig. 6c). The lack of interaction in the presence of both nucleotides might indicate that the high-affinity complex is asymmetric regarding the nucleotide bound in the NBDs of Hsc70 and Apg2, that is, Hsc70 is in the ADP or apo conformation, while Apg2 is bound to ATP. This hypothesis is supported by the crystal structures of Hsp70:Hsp110 complexes [19,20]. We observed complex formation when both proteins were in their apo forms, states with the inherent conformational flexibility required for the interaction. The equilibrium

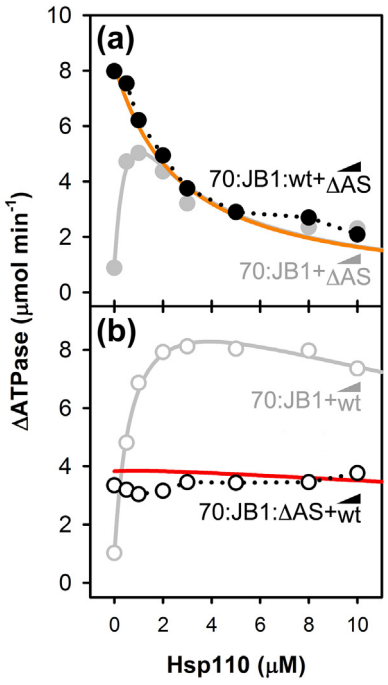

Fig. 7. Apg2 and Apg2ΔAS regulate the ATPase of Hsc70 system following similar mechanics. (a) ATPase activity of Hsc70 (2 μM) in the presence of DnaJB1 (0.5 μM) and wt Apg2 (3 μM), measured at increasing concentrations of Apg2ΔAS (black circles). For comparison, the activities obtained in the absence of wt Apg2 are shown (gray circles). ΔATPases were obtained subtracting the basal activity of Apg2ΔAS at each protein concentration. (b) Activity measurements as in panel a, using Hsc70 (2 μM), DnaJB1 (0.5 μM) and Apg2ΔAS (3 μM) and increasing concentrations of wt Apg2 (white circles). Similarly, the curve obtained in the absence of Apg2ΔAS is shown (gray circles). The gray lines in panels a and b represent the best fit to the phenomenological model [Eq. (1)] for Apg2ΔAS and wt Apg2, respectively. The common values of the parameters are $R_0 = 0.543\ \text{min}^{-1}$, $C_R = 8.26\ \mu\text{M}^{-1}\ \text{min}^{-1}$ and $T_0 = 0.181$ min. The value of C_T is $0.101\ \mu\text{M}^{-1}$ min for Apg2ΔAS and $0.0077\ \mu\text{M}^{-1}$ min for wt Apg2. The orange and red lines represent the prediction of the model for the competition experiments using additive effects with the parameters above, as described in the main text.

binding constants for the apo forms were determined from plots of the maximal RUs obtained at increasing concentrations of the injected protein, resulting in K_D values of 148 ± 5 and 54 ± 1 nM for wt Apg2 and Apg2ΔAS, respectively (Fig. 6c). To gain a better insight on how the AS might regulate the affinity of Apg2 for Hsc70, we performed similar SPR experiments with the Hsc70 NBD (residues 1 to 384). The 3D structures of Hsp70:Hsp110 complexes show that Hsp110 establishes extensive contacts with the Hsp70 NBD, while its SBD is positioned in the vicinity of Hsp110 SBD-β where the AS is located [19,20]. First, we observed that after deletion of Hsc70 SBD, the affinity for wt Apg2 is strongly reduced from 148 to 1800 nM, which might suggest that contacts between the SBDs of both proteins are involved in complex formation, or that disruption of the Hsc70 allosteric interface modifies the interaction. Second, the 3-fold affinity increase for Hsc70 observed with the deletion mutant was not found for the isolated NBD domain of Hsc70, the K_D values being 1.8 ± 0.2 and 1.3 ± 0.2 μM for wt Apg2 and Apg2ΔAS, respectively (Fig. 8c). Therefore, these results indicate that the AS of Apg2 regulates the affinity for Hsc70 possibly through interactions with its SBD that modify the allosteric interface. To discard that a disordered region of Apg2 might act as a pseudosubstrate for Hsc70 and thus contribute to the overall affinity, as occurs in the bacterial system [37,38], the SPR experiments were performed with the Hsc70 V438F mutant. Resembling DnaK V436F [39], Hsc70 V438F was unable to bind FYQLALT with high affinity (Supplementary Fig. S5D). We observed a slight increase of the K_D values to 238 ± 11 and 101 ± 14 nM for wt Apg2 and Apg2ΔAS, respectively, indicating that the pseudosubstrate interaction proposed above does not induce a significant affinity gain and is not modulated by the AS. This interpretation is further supported by the finding that Hsc70:Apg2 complex formation does not alter the peptide binding site of the chaperone (Table 1 and Supplemental Fig. S3).

Discussion

Protein aggregate reactivation in metazoa (human) depends on the activity of Hsp70/Hsp40/Hsp110 chaperones. The chaperoning activity of Hsp70 proteins involves substrate binding and release cycles that are optimally regulated by ATP hydrolysis and cochaperones. In the ATP conformation, Hsp70 interacts with polypeptides with fast association and dissociation kinetics. Unfolded, misfolded and aggregated protein substrates are presented to Hsp70 by Hsp40 cochaperones that synergistically with the substrate stimulate ATP hydrolysis. The conformational changes brought about by nucleotide hydrolysis favor substrate trapping in the ADP conformation. NEFs facilitate ADP/ATP exchange and release of the substrate, initiating the refolding process. Hsp110 proteins behave as essential NEFs in the reactivation of protein aggregates in metazoans, other cytosolic NEFs as Bag1 being unable to support it [4,5]. Interestingly, in contrast to the human Hsc70/DnaJB1/Apg2 chaperone system, the yeast homologs Ssa1/Ydj1/Sse1 cannot support refolding of protein aggregates in similar conditions and rely on the potent disaggregase activity of Hsp104 [5]. Among the differences between the human and yeast chaperones, the sequence evolution of the Hsp110 stands out, being the human representatives larger due to the extension of the C-terminus and the characteristic acidic sequence inserted in the SBD-β [1,2]. We find here that deletion of this acidic insertion, which we termed AS, is involved in the regulation of Hsc70

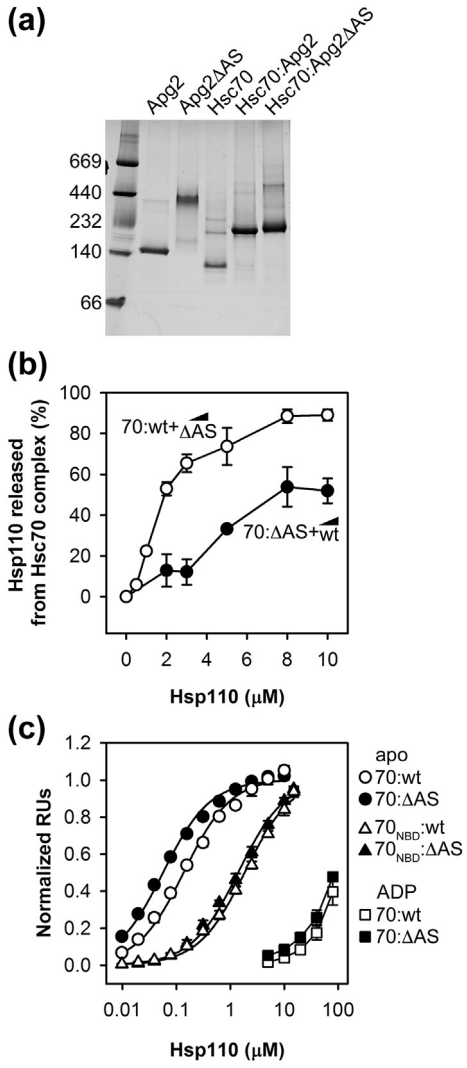

Fig. 8. Deletion of the AS increases the affinity of Apg2 for Hsc70. (a) Native electrophoresis of the different proteins and protein complexes used in this study. (b) Release of wt Apg2 (white circles) and Apg2ΔAS (black circles) from their corresponding complexes with Hsc70 at increasing concentrations of Apg2ΔAS and wt Apg2, respectively. The average of three different experiments is shown. (c) Binding curves of Apg2 (white symbols) and Apg2ΔAS (black symbols) to Hsc70 (circles) and Hsc70 NBD (triangles) in the absence of nucleotides derived from SPR analysis. The interaction of Apg2 and Apg2ΔAS with Hsc70 was also studied in the presence of purified ADP (squares). Normalized maximal resonance units (RU) were obtained at different concentrations of wt Apg2 (white symbols) and Apg2ΔAS (black symbols). Fitting of the curves to a single site binding model (black lines) yielded dissociation constants of 148 ± 5 and 54 ± 1 nM for the interaction of wt Apg2 and Apg2ΔAS with Hsc70, respectively. The same analysis for complex formation with the Hsc70 NBD gave K_D values of 1.8 ± 0.2 and 1.3 ± 0.2 μM for wt Apg2 and Apg2ΔAS, respectively.

activity as it increases the affinity of Apg2 for Hsc70, inhibits the cochaperone-induced ATPase stimulation of Hsc70, impairs Hsc70 recruitment to the surface of aggregated substrates and its subsequent reactivation. Interestingly, several members of the Hsp110 family express isoforms in which the AS domain is partially deleted as in human and mouse Hsp105 (isoforms β), and fly Hsc70Cb (isoform A). In humans, Hsp105β is mainly expressed in the nucleus due to the lack of a sorting signal located in the AS [21,22]. The role of this isoform with a shortened AS in nuclear protein homeostasis is unknown. This protein subdomain is also the target of several post-translational modifications, found in different high-throughput studies in both Apg2 and Hsp105 (Supplemental Table 2). Future work should address how these modifications in the AS might modulate the Hsc70 system activity and its interaction with protein substrates.

The functional defects described above are concentration dependent and are observed above 0.2–0.4 μM Apg2ΔAS (Fig. 9a). Importantly, the reduction of the ATPase activity, Hsc70 binding to aggregates and refolding activity is not due to the truncation of the AS since they are also observed for wt Apg2, although at higher concentrations, for example, a similar inhibition of aggregate reactivation was observed at approximately 3- to 4-fold higher concentration for the wt protein. In agreement with our data, elevated concentrations of human Hsp105 also reduced Hsc70 ATPase activity [27,32]. Our phenomenological model characterizes in quantitative detail the effects of the AS as a regulatory element of the Hsc70 ATPase cycle, showing that this protein region is not involved in the catalytic activity of Apg2, as it does not affect the nucleotide exchange, but slows down 10 times the ATPase cycle compared to the wt. The fact that the NEF-induced inhibition of the ATPase and chaperone activities can be counteracted by higher DnaJB1 concentrations suggests that the fitness of the Hsc70 system depends on the cochaperone molar ratio. Similarly, unbalance of the DnaJ/GrpE ratio induced important detrimental effects on the chaperone activity of the bacterial DnaK system [33–35,40,41]. Therefore, our results show that the human Hsc70 system follows a similar pattern to the bacterial one, in which the balance of DnaJB1 and Apg2 cochaperones regulates *in vitro* the correct timing of the Hsc70 cycle required for optimal function. The maintenance of the Hsc70 system functionality *in vivo* is ensured by a strict regulation of cochaperone concentrations, the amount of Hsp110 proteins being approximately equal to that of Hsp40s under normal conditions, and less abundant after heat shock [9,42].

Our data demonstrate that the AS of Apg2 plays an important role in the chaperone activity of Hsc70 as deletion of this domain significantly narrows the Apg2 concentration range that leads to reactivation of protein substrates. The outcome of the reactivation reaction also depends on the conformational

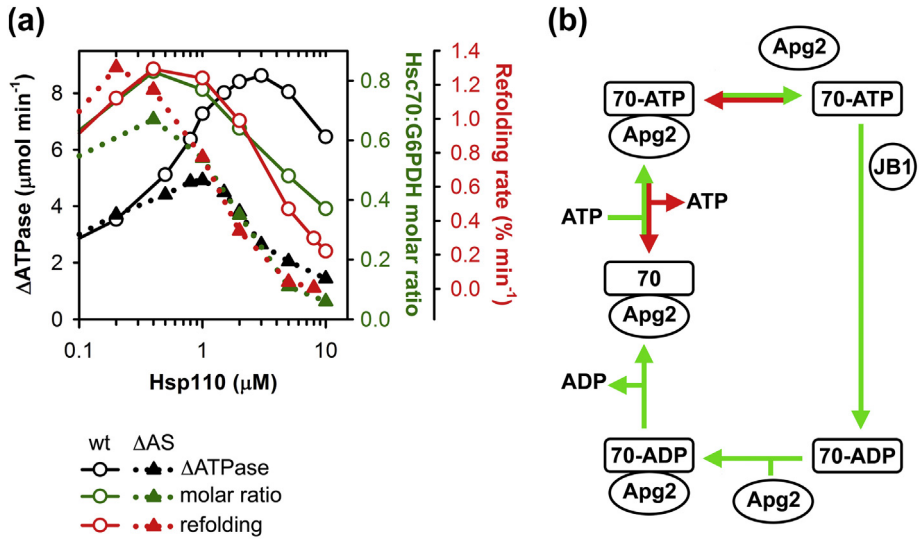

Fig. 9. Regulation of ATPase, Hsc70 binding to aggregates and their refolding by Apg2. (a) Comparison of the ATPase activity (black), Hsc70 binding to G6PDH aggregates (green) and their refolding (red) at increasing concentrations of Apg2 and Apg2ΔAS. Data were taken from Figs. 2c, 3d and 5a. Open circles and continuous lines represent the experimental values for wt Apg2 and closed triangles and dotted lines for Apg2ΔAS. (b) Schematic model of Hsc70 system ATPase cycle. Stimulation of ATP hydrolysis by DnaJB1 and nucleotide exchange by Apg2 contribute positively to the steady-state ATPase (green arrows). Red arrows represent the negative contribution of Apg2 to the cycle due to binding to Hsc70(ATP) that might promote dissociation of the nucleotide before hydrolysis.

properties of the substrates. The 30% reduction in the recovery of denatured luciferase hold in a folding-competent conformation by 2 μM Apg2ΔAS agrees well with results found for a yeast Sse1 variant that lacks the smaller acidic loop [19]. Reactivation of aggregates is severely diminished by Apg2ΔAS at 2 μM: the reduction varies from 3-fold for mild aggregates (chemically denatured luciferase and G6PDH aggregates formed at 50 °C), to almost zero reactivation for stable aggregates (thermally denatured luciferase). This suggests that the fitness of the Hsc70 system is essential to perform challenging tasks as aggregate reactivation in which the extraction of unfolded polypeptides requires chaperone-mediated disruption of strong intermolecular interactions that stabilize the aggregate [28,43,44]. We find a straight correlation between the effect of both Apg2 and Apg2ΔAS on the refolding activity and the amount of Hsc70 bound to the aggregate (Fig. 9a), suggesting that the limiting step is the extraction of polypeptides as previously suggested [28,45]. Our results show that the interaction of Hsc70 with aggregates depends on both cochaperones, as DnaJB1 increases 5-fold the amount of Hsc70 associated with the aggregate, similarly to what has been described for the bacterial DnaK system [43], and inclusion of 0.4 μM Apg2 induces a further 2-fold increase, a novel finding in this work. The amount of aggregate-bound Hsc70 is reduced when the concentration of wt Apg2 and, more markedly, Apg2ΔAS increases, as expected from the refolding results. Although Apg2 can interact with high affinity with hydrophobic peptides and unfolded substrates ([46] and this work), its affinity for G6PDH aggregates seems to be remarkably lower. The amount of aggregate-bound Apg2 remained constant (approx. 2% of the initially added protein) even at high NEF concentrations when Hsc70 binding strongly decreased, especially for the truncation mutant, suggesting that the chaperone does not occupy potential binding sites for Apg2. The Apg2:Hsc70 molar ratio at the aggregate surface is 1:80 when refolding is maximum, suggesting a catalytic role for Apg2 in the extraction of unfolded polypeptides from the aggregate, which would favor a specialized NEF function over a mechanical activity related to the extraction of aggregated chains in cooperation with Hsc70 [5,14].

According to our data and work done with human Hsp105 [27,32], the main difference between Hsp110s and other unrelated NEFs regarding the regulation of Hsc70 resides in the regulation of the ATPase activity. Human Bag1, HspBP1 and bacterial GrpE stimulate the ATPase activity of Hsc70 and DnaK reaching saturation in a concentration range similar to that used here [27,34,41,47,48]. These NEFs also reduce the refolding activity of the complete system, an effect that has been attributed to modifications of the time the substrate remains bound to Hsp70 [41,48]. However, Rauch and Gestwicki [49] described that different Bag proteins combined with a set of Hsp40s (including DnaJB1) induced a strong inhibition of Hsp72 (HspA1A) in the 0- to 4-μM range. Moreover, the authors observed

that Hsp105 was unable to activate Hsp72, in contrast to Hsc70 [27,32,50]. These discrepancies suggest that specific properties of Hsc70 (HspA8) and Hsp72 (HspA1A) determine how their activity is modulated by different combinations of NEF/Hsp40 cochaperones. HspA8 and HspA1A might require a different regulation when performing their respective roles as the constitutive and the main stress-inducible members of the Hsp70 family. Tuning down both the ATPase and refolding activity of HspA1A under stress could be beneficial for the cell to avoid ATP depletion, promoting the required holdase activity. This regulation is well known in bacteria and mitochondria where DnaK and mtHsp70 are modulated by the reversible unfolding of their NEFs, GrpE and Mge1p [51,52]. Regulation of Hsp70s in the eukaryotic cytosol is more complex due to the coexistence of different Hsp70s and the plethora of cochaperones available. The properties of specific Hsp70s and the combination and stoichiometry of the NEF/Hsp40 cochaperone pair might be essential to regulate the activity of the system in different environmental conditions.

The question that remains is how Apg2 inhibits the ATPase cycle of Hsc70 at high concentration. Due to the role of Apg2 as a NEF of Hsc70, the most reasonable point to arrest the cycle would be the ADP/ATP exchange process, basically consisting of the following: binding of Apg2 to Hsc70(ADP), ADP dissociation, and ATP binding and dissociation of the complex (Fig. 9b). Neither formation of the Hsc70(ADP):Apg2 complex nor dissociation of ADP could reduce the ATPase rates: first, complex formation would be favored at high Apg2 concentration, and second, we found that ADP exchange rates increase and saturate. Since the dissociation of the Hsc70:Apg2 complex upon ATP binding is inherently concentration independent, a reasonable explanation could be that Apg2 re-associates to Hsc70(ATP), a binding event favored at high concentration, and promotes the premature release of ATP before hydrolysis as Raviol *et al.* [36] showed, delaying the progression of the ATPase cycle. This hypothesis is in line with the stronger inhibitory effect observed for Apg2ΔAS coupled to the increased affinity of the mutant for Hsc70 and suggests an important role for the AS to avoid complex re-association. While ADP dissociation rates reach maximum values within the concentration range studied, ATP dissociation might increase at high NEF concentration, resulting in the biphasic behavior of the steady-state ATPase. Thus, Apg2 and DnaJB1 will compete to bind Hsc70(ATP), promoting the stimulation of the chaperone cycle and activity at low Apg2:DnaJB1 ratios, while increasing Apg2 concentration would favor ATP dissociation and inhibition of the system. High Apg2 concentration would also promote faster ADP/ATP exchange rates, reducing the time the substrates remain bound to the chaperone. However, dissociation of ATP from Hsc70 would populate conformations able to re-bind peptides that were previously released by ATP binding, an interaction possibly favored by the local peptide concentration, resulting in the slower peptide dissociation kinetics. It would also reduce chaperone binding to aggregates by decreasing the population of Hsc70(ATP), the conformation competent to be recruited by aggregate-bound DnaJB1. This links aggregate binding and reactivation to the inhibition of the steady-state ATPase activity, although a direct correlation with the absolute ATPase value is not observed (Fig. 9a), possibly due to the counteracting effect of DnaJB1 in solution and differences in the association kinetics of Apg2 to Hsc70(ADP) and Hsc70 (ATP), on which nucleotide exchange and ATP dissociation would depend, respectively. Deletion of the AS does not modify nucleotide exchange, but its higher affinity for Hsc70 facilitates association to Hsc70 (ATP) decreasing its population more efficiently than wt Apg2 and therefore the chaperone ability to interact with aggregates.

Mechanistically, it is difficult to understand how the AS regulates the interaction between Hsc70 and Apg2, due to the lack of structural information of this protein subdomain [18–20]. In the complex, the Hsp70 NDB establishes extensive contacts with the NBD and SBD-α of Hsp110, while the SBD of bovine Hsc70 positions in the vicinity of the Sse1 SBD-β without contacting it [19,20]. In all the structures, the AS seems to be far from the NBD of Hsp70 in the heterocomplex but close to the SBD and does not participate in the interaction interface. Upon deletion of Apg2 AS, the affinity for Hsc70 increases 3-fold for full-length Hsc70 but not for its NBD, suggesting that the AS interacts with Hsc70 SBD. Importantly, deletion of Hsc70 SBD has a great impact in the K_D of the complex with wt Apg2 that is increased 1 order of magnitude (from 0.14 to 1.8 μM), as found for yeast Ssa1p and Sse1p, albeit to a lower extent (K_D increased from 0.1 to 0.4 μM after deletion of Ssa1p SBD) [19,36]. These results indicate that both domains of Hsc70 and their allosteric interface are essential to bind Apg2 with high affinity. An interaction of the AS, plausibly with Hsc70 SBD, might destabilize the Hsc70:Apg2 complex modulating Hsc70 allosterism. Similarly, we have described that the interaction between bacterial DnaK SBD and the long N-terminal tail of GrpE has important effects in the regulation and plasticity of the complex [38,53]. This type of multivalent contacts could help the NEFs to better tune the conformational rearrangements during the functional cycle of their Hsp70 counterparts. The lack of significant ATP-induced conformational transitions in Hsp110 proteins [24,54,55] makes difficult to establish the role of the AS in the complex allosteric cycle of the Hsc70 system, but our data suggest that it might serve as a molecular switch to

avoid re-association of the Hsc70:Hsp110 complex and facilitate progression of the chaperone cycle.

Materials and Methods

Cloning, expression and purification of proteins

The cDNAs of Apg2 (HSPH2), Hsc70 (HSPA8) and DNAJB1 were obtained from Addgene and cloned into pE-SUMO vector (LifeSensors). The mutant Apg2ΔAS, carrying a deletion from residue 504 to 569, was cloned by fusing two PCR fragments corresponding to the upstream and downstream sequences of these protein segments. Hsc70 V438F was obtained by the Quick-change protocol (Agilent). Recombinant proteins containing a tag with 6 histidines and SUMO fused to the N-terminus were expressed in BL21 Rossetta cells and purified with a first step of affinity chromatography using NiNTA (Quiagen) columns, followed by treatment with the protease Ulp1 to cleave the tag, and a final NiNTA column in which the pure protein eluted in the unbound fraction. For Hsc70, Hsc70 V438F and the NBD mutant (residues 1–384), an additional polishing step with a hydroxyapatite column was performed.

Small-angle X-ray scattering measurements

Synchrotron X-ray diffraction data for recombinant purified Apg2 and Apg2ΔAS were collected on a pixel Pilatus 2M detector at Diamond Light Source B21 beamline (UK). The scattering patterns were measured with a 2-s exposure time per frame in a continuous mode using an in-line Agilent HPLC system connected to a SHODEX PROTEIN KW403-4F column (exclusion limit of 600 kDa) equilibrated in 40 mM Hepes (pH 7.6), 50 mM KCl, 5 mM $MgCl_2$ and 2 mM DTT and running at 0.16 ml min^{-1}. To check for radiation damage, the accumulated frames corresponding to eluted peaks were compared as a time series and no radiation damage was observed. Using the sample-to-detector distance of 4.01 m, the range of momentum transfer values is $0.0025 < q < 0.42$ $Å^{-1}$ ($q = 4\pi\sin(\theta)/\lambda$, where 2θ is the scattering angle and $\lambda = 1$ Å is the X-ray wavelength). Data were processed using standard procedures by the program packages ScÅtter (developed by Rob Rambo at Diamond Light Source) and PRIMUS [56]. The forward scattering ($I(0)$) was evaluated using the Guinier approximation [57], assuming that the intensity is represented as $I(q) = I(0)\exp(-(qR_g)^2/3)$ for a very small range of momentum transfer values ($q < 1.3/R_g$). The maximum dimensions (D_{max}), the interatomic distance distribution functions ($P(r)$), and the radii of gyration (R_g) were computed using GNOM [58]. The molecular mass of the protein was evaluated with the equation $ln\ (Q_R) = k * ln\ (\text{Mass}) + c$, where $Q_R = (V_c^2/R_g)$, and k and c are constants [59] (Table S1).

Ab initio shape determination and *in silico* Apg2 molecular modeling

The *ab initio* reconstructions of Apg2 and Apg2ΔAS were calculated using GASBOR [60] and MONSA [61]. Representative *ab initio* reconstructions were selected based on DAMCLUST [62]. A 3D molecular model of Apg2 was generated combining homology modeling using Phyre2 [63], *de novo* peptide structure prediction by PEP-FOLD3 [64] and SAXS refinement by SREFLEX [65]. A search for structural homologs predicted residue ranges 1–512 and 570–702 in Apg2 (missing the AS and C-terminal region) are related to the 3D crystal structure of *S. cerevisiae* heat shock protein homolog Sse1p (PDB code 3D2F; sequence identity 42%). Also, Apg2 residue range 703–785 was predicted to be homologous to the C-terminal 10-kDa subdomain of *Caenorhabditis elegans* heat shock 70 kDa protein A Hsp70 (PDB code 2P32; sequence identity 25%). Given that no convincing homologs were found for residues 513–569, corresponding to the AS, and the C-terminal residues 786–840, *de novo* peptide structure prediction was used instead. A first 3D molecular model of Apg2 was assembled using the fragments obtained and taking into account the *ab initio* envelope reconstructions previously determined by MONSA, followed by several rounds of refinement against the experimental SAXS data in SREFLEX.

Refolding of unfolded luciferase

Luciferase (0.1 μM) was denatured by incubation at 42 °C for 30 min in the absence or the presence of Apg2 or Apg2ΔAS at 0.4 or 2 μM in 40 mM Hepes (pH 7.6), 50 mM KCl, 5 mM $MgCl_2$, 2 mM DTT, 2 mM ATP, 3 mM PEP and 20 ng/ml pyruvate kinase. Samples were incubated for 5 min at 30 °C, and refolding was initiated by addition of Hsc70 (2 μM) and DnaJB1 (1 μM). Luciferase activity was measured after 1 h in a Synergy HTX plate reader (Biotec), using E1500 assay buffer (Promega). The activity of luciferase diluted in the above buffer containing chaperones at final concentration and incubated at 30 °C for the length of the experiment was set to 100%.

Refolding of luciferase and G6PDH aggregates

Luciferase (2 μM) was incubated at 30 °C for 30 min in denaturation buffer [6 M urea, 40 mM Hepes (pH 7.6), 50 mM KCl, 5 mM $MgCl_2$, 2 mM DTT]. Aggregation was induced by 100-fold dilution into refolding buffer [40 mM Hepes (pH 7.6), 50 mM KCl, 5 mM $MgCl_2$, 2 mM DTT, 2 mM ATP, 3 mM PEP, 20 ng/ml pyruvate kinase]. Reactivation was started by the addition of chaperones: 2 μM Hsc70, 1 μM DnaJB1, 0–8 μM Apg2 or Apg2ΔAS. Final luciferase concentration was 20 nM. G6PDH (glucose-6-phosphate dehydrogenase) aggregates (2.5 μM) were formed after incubation at 50 °C for 30 min in

50 mM Tris–HCl (pH 7.5), 150 mM KCl, 20 mM $MgCl_2$ and 10 mM DTT diluted to 0.4 μM in refolding buffer and preincubated at 30 °C for 10 min before the addition of chaperones at the concentrations indicated above. To monitor reactivation of luciferase aggregates, the activity of aliquots taken at different times during 2 h was determined as above. G6PDH activity was measured as described [66]. Reactivation rates were obtained from the linear regression of the initial part of the refolding kinetic, as previously described [67].

Interaction with G6PDH aggregates

G6PDH aggregates (10 μM) were formed after incubation at 50 °C for 30 min in 50 mM Tris (pH 7.4), 150 mM KCl, 20 mM $MgCl_2$ and 10 mM DTT. Temperature was lowered to 30 °C for 10 min and G6PDH aggregates were diluted to 1 μM in 40 mM Hepes (pH 7.6), 50 mM KCl, 5 mM $MgCl_2$, 2 mM DTT, 2 mM ATP, 8 mM PEP and 20 ng/μl PK buffer, containing Hsc70 (2 μM), DnaJB1 (0.5 μM) and increasing concentrations of Apg2 or Apg2ΔAS. Chaperones were preincubated 5 min at 30 °C in the above buffer before aggregate addition. After 10-min incubation, the samples were centrifuged at 55.000 rpm in a TLA-55 rotor (Beckman) at 4 °C. Proteins in pellets were analyzed and quantified by SDS-PAGE and densitometry. The amount of chaperones precipitated in the presence of native G6PDH (controls) was averaged from at least three experiments and subtracted from that sedimented with the aggregates. ODs are converted to μg of protein using references lines containing 1 μg of each protein. We have checked that this simple calculation guesses quite correctly the amount of protein compared to in-gel calibration curves.

Peptide binding and release kinetics

Kinetics of substrate interaction with Hsc70 have been measured using the peptide FYQLALT labeled with the fluorescent probe TAMRA (Proteogenix, Schiltigheim, France). Binding was assayed adding 0.1 μM t-FYQLALT to Hsc70 or its complexes with Apg2 or Apg2ΔAS at 2, 4, 6 and 8 μM. Complexes were preformed by overnight incubation in 40 mM Hepes (pH 7.6), 50 mM KCl, 5 mM $MgCl_2$, 2 mM DTT and 50 μM ATP at 25 °C. Peptide release was induced by adding 0.2 mM ATP and different concentrations of Apg2 or Apg2ΔAS to preformed Hsc70:t-FYQLALT complexes, obtained after 3-h incubation of 1 μM Hsc70 and 0.5 μM t-FYQLALT in 40 mM Hepes (pH 7.6), 50 mM KCl, 5 mM $MgCl_2$, 2 mM DTT and 0.1 mM ADP at 25 °C. The anisotropy of the sample was continuously measured to characterize binding and release kinetics in a SLM8100 (Aminco) spectrofluorimeter, using 555- and 580-nm excitation and emission wavelengths, respectively, and 8 × 8 slits.

ATPase measurements

Steady-state ATPase activity was measured using the assay described by Norby [68]. Assays were performed at 30 °C in 40 mM Hepes (pH 7.6), 50 mM KCl, 5 mM Mg acetate and 1 mM ATP. Protein concentrations were 2 μM Hsc70, 0–2 μM DnaJB1, 0–10 μM Apg2 or Apg2ΔAS as indicated. Reactions were monitored by continuously measuring the absorbance decay at 340 nm for 1 h in a Synergy HTX plate reader (Biotec).

Nucleotide exchange

Nucleotide exchange kinetics was measured in an SFM 300/MOS 450 Stopped-flow machine (BioLogic, Grenoble, France) using MABA fluorescence. Upon excitation at 365 nm, emission selected with a 400-nm cutoff filter. The average mixing time of the experiment was 80 ms. The cell chamber and container syringes were kept at 25 °C. Hsc70-MABA-ADP complex was mixed with ADP in the presence of increasing concentrations of Apg2 or Apg2ΔAS to obtain final reactants concentrations: 0.48 μM Hsc70-MABA, 268.5 μM ADP, and 0 to 3 μM Hsp110 in 40 mM Hepes (pH 7.6), 50 mM KCl and 5 mM $MgCl_2$. MABA release was recorded immediately after mixing as a decrease in its fluorescence signal. Kinetic constants were calculated by fitting the experimental traces to a mono-exponential transition by means of the Bio-Kine32 v4.65 analysis software provided by Biologic.

Native gel electrophoresis

Hsc70:Apg2 or Hsc70:Apg2ΔAS complexes were prepared by mixing 2 μM of each protein in the presence of 50 μM of ATP in 40 mM Hepes (pH 7.6), 50 mM KCl, 5 mM $MgCl_2$ and 2 mM DTT and overnight incubation at room temperature. Complexes were resolved by native PAGE using 4%–16% Bis–Tris gels (Invitrogen). Competition experiments were set up adding the competing Hsp110 to the corresponding incubation mixture at 0.5, 1, 2, 3, 5, 8 and 10 μM. Free Apg2 or Apg2ΔAS was analyzed by densitometry.

Surface plasmon resonance spectroscopy (SPR)

SPR assays were performed in a Biacore 3000 system (GE Healthcare). Hsc70 carrying a C-terminal strep-tag II was bound to a CM5 chip (GE Healthcare), in which the monoclonal antibody StrepMAB-Immo (IBA Lifesciences), raised against the strep-tag II sequence, was previously immobilized using the amine coupling kit supplied by GE Healthcare. Apg2 and Apg2ΔAS were dialyzed overnight at 4 °C in running buffer [40 mM Hepes (pH 7.5), 150 mM KCl, 5 mM $MgCl_2$ and 0.0025%

Tween 20] prior to 1-min injection at concentrations from 0.01 to 10 μM. After every injection, 1 M NaCl was passed through the flow cells for 1 min to wash away Hsp110 remainders that might not have dissociated. Measurements were done at 25 °C and at a flow rate of 30 μl/min. For the experiments in the presence of nucleotides, 2 mM ATP or purified ADP [69] was added. Double subtraction of buffer and control lane (injection of Apg2 or Apg2ΔAS along a flow cell without Hsc70) was performed. K_D values were determined by plotting maximal RUs achieved *versus* Hsp110 concentration and fitting the data to a hyperbolic ligand-binding equation.

Acknowledgements

We thank to N. Orozco for excellent technical support. Y.C. and L.D. are recipients of UPV/EHU and MEC FPU predoctoral fellowships, respectively. We acknowledge Diamond Light Source (proposals mx15304), SOLEIL (proposal 20150773) and iNEXT (proposals 1618/2538) for providing access to synchrotron radiation facilities. This work was supported by the MINECO Contract BFU2016-77427-C2-2-R and Severo Ochoa Excellence Accreditation (SEV-2016-0644) to M.E.G., FIS2015-68722-R (MICINN/FEDER) to J.M.G.V., and IT709-13 (Basque Government) and MINECO BFU2016-75983-P (AEI/FEDER, UE) to A.M. and F.M.

Appendix A. Supplementary data

Supplementary data to this article can be found online at https://doi.org/10.1016/j.jmb.2018.11.026.

Received 16 July 2018;
Received in revised form 30 October 2018;
Accepted 26 November 2018
Available online 4 December 2018

Keywords:
Apg2;
Hsp110;
Hsc70;
chaperone complex;
aggregate reactivation

Abbreviations used:
AS, acidic subdomain; NEF, nucleotide exchange factor; 70, Hsc70; JB1, DnaJB1; wt, wt APG2; ΔAS, Apg2ΔAS deletion mutant; G6PDH, glucose 6-phosphate dehydrogenase; NBD, nucleotide binding domain; SBD, substrate binding domain.

References

[1] A. Aguado, J.A. Fernandez-Higuero, F. Moro, A. Muga, Chaperone-assisted protein aggregate reactivation: different solutions for the same problem, Arch. Biochem. Biophys. 580 (2015) 121–134.
[2] N.B. Nillegoda, B. Bukau, Metazoan Hsp70-based protein disaggregases: emergence and mechanisms, Front. Mol. Biosci. 2 (2015) 57.
[3] A. Mogk, B. Bukau, H.H. Kampinga, Cellular handling of protein aggregates by disaggregation machines, Mol. Cell 69 (2018) 214–226.
[4] J. Shorter, The mammalian disaggregase machinery: Hsp110 synergizes with Hsp70 and Hsp40 to catalyze protein disaggregation and reactivation in a cell-free system, PLoS One 6 (2011), e26319.
[5] H. Rampelt, J. Kirstein-Miles, N.B. Nillegoda, K. Chi, S.R. Scholz, R.I. Morimoto, et al., Metazoan Hsp70 machines use Hsp110 to power protein disaggregation, EMBO J. 31 (2012) 4221–4235.
[6] N.B. Nillegoda, J. Kirstein, A. Szlachcic, M. Berynskyy, A. Stank, F. Stengel, et al., Crucial HSP70 co-chaperone complex unlocks metazoan protein disaggregation, Nature 524 (2015) 247–251.
[7] D.P. Easton, Y. Kaneko, J.R. Subjeck, The hsp110 and Grp1 70 stress proteins: newly recognized relatives of the Hsp70s, Cell Stress Chaperones 5 (2000) 276–290.
[8] D. Lee-Yoon, D. Easton, M. Murawski, R. Burd, J.R. Subjeck, Identification of a major subfamily of large hsp70-like proteins through the cloning of the mammalian 110-kDa heat shock protein, J. Biol. Chem. 270 (1995) 15725–15733.
[9] J. Hageman, M.A. van Waarde, A. Zylicz, D. Walerych, H.H. Kampinga, The diverse members of the mammalian HSP70 machine show distinct chaperone-like activities, Biochem. J. 435 (2011) 127–142.
[10] Z. Dragovic, S.A. Broadley, Y. Shomura, A. Bracher, F.U. Hartl, Molecular chaperones of the Hsp110 family act as nucleotide exchange factors of Hsp70s, EMBO J. 25 (2006) 2519–2528.
[11] C. Andreasson, J. Fiaux, H. Rampelt, M.P. Mayer, B. Bukau, Hsp110 is a nucleotide-activated exchange factor for Hsp70, J. Biol. Chem. 283 (2008) 8877–8884.
[12] H.J. Oh, X. Chen, J.R. Subjeck, Hsp110 protects heat-denatured proteins and confers cellular thermoresistance, J. Biol. Chem. 272 (1997) 31636–31640.
[13] H.J. Oh, D. Easton, M. Murawski, Y. Kaneko, J.R. Subjeck, The chaperoning activity of hsp110. Identification of functional domains by use of targeted deletions, J. Biol. Chem. 274 (1999) 15712–15718.
[14] R.U. Mattoo, S.K. Sharma, S. Priya, A. Finka, P. Goloubinoff, Hsp110 is a bona fide chaperone using ATP to unfold stable misfolded polypeptides and reciprocally collaborate with Hsp70 to solubilize protein aggregates, J. Biol. Chem. 288 (2013) 21399–21411.
[15] A. Saxena, Y.K. Banasavadi-Siddegowda, Y. Fan, S. Bhattacharya, G. Roy, D.R. Giovannucci, et al., Human heat shock protein 105/110 kDa (Hsp105/110) regulates biogenesis and quality control of misfolded cystic fibrosis transmembrane conductance regulator at multiple levels, J. Biol. Chem. 287 (2012) 19158–19170.
[16] J. Wang, G.W. Farr, C.J. Zeiss, D.J. Rodriguez-Gil, J.H. Wilson, K. Furtak, et al., Progressive aggregation despite chaperone associations of a mutant SOD1-YFP in transgenic mice that develop ALS, Proc. Natl. Acad. Sci. U. S. A. 106 (2009) 1392–1397.

[17] H. Yamashita, J. Kawamata, K. Okawa, R. Kanki, T. Nakamizo, T. Hatayama, et al., Heat-shock protein 105 interacts with and suppresses aggregation of mutant Cu/Zn superoxide dismutase: clues to a possible strategy for treating ALS, J. Neurochem. 102 (2007) 1497–1505.
[18] Q. Liu, W.A. Hendrickson, Insights into Hsp70 chaperone activity from a crystal structure of the yeast Hsp110 Sse1, Cell 131 (2007) 106–120.
[19] S. Polier, Z. Dragovic, F.U. Hartl, A. Bracher, Structural basis for the cooperation of Hsp70 and Hsp110 chaperones in protein folding, Cell 133 (2008) 1068–1079.
[20] J.P. Schuermann, J. Jiang, J. Cuellar, O. Llorca, L. Wang, L. E. Gimenez, et al., Structure of the Hsp110:Hsc70 nucleotide exchange machine, Mol. Cell 31 (2008) 232–243.
[21] Y. Saito, N. Yamagishi, T. Hatayama, Different localization of Hsp105 family proteins in mammalian cells, Exp. Cell Res. 313 (2007) 3707–3717.
[22] Y. Saito, N. Yamagishi, T. Hatayama, Nuclear localization mechanism of Hsp105beta and its possible function in mammalian cells, J. Biochem. 145 (2009) 185–191.
[23] L. Shaner, A. Trott, J.L. Goeckeler, J.L. Brodsky, K.A. Morano, The function of the yeast molecular chaperone Sse1 is mechanistically distinct from the closely related hsp70 family, J. Biol. Chem. 279 (2004) 21992–22001.
[24] H. Raviol, B. Bukau, M.P. Mayer, Human and yeast Hsp110 chaperones exhibit functional differences, FEBS Lett. 580 (2006) 168–174.
[25] S. Polier, F.U. Hartl, A. Bracher, Interaction of the Hsp110 molecular chaperones from *S. cerevisiae* with substrate protein, J. Mol. Biol. 401 (2010) 696–707.
[26] K. Gotoh, K. Nonoguchi, H. Higashitsuji, Y. Kaneko, T. Sakurai, Y. Sumitomo, et al., Apg-2 has a chaperone-like activity similar to Hsp110 and is overexpressed in hepatocellular carcinomas, FEBS Lett. 560 (2004) 19–24.
[27] S. Tzankov, M.J. Wong, K. Shi, C. Nassif, J.C. Young, Functional divergence between co-chaperones of Hsc70, J. Biol. Chem. 283 (2008) 27100–27109.
[28] S.P. Acebron, I. Martin, U. del Castillo, F. Moro, A. Muga, DnaK-mediated association of ClpB to protein aggregates. A bichaperone network at the aggregate surface, FEBS Lett. 583 (2009) 2991–2996.
[29] B. Gao, L. Greene, E. Eisenberg, Characterization of nucleotide-free uncoating ATPase and its binding to ATP, ADP, and ATP analogues, Biochemistry 33 (1994) 2048–2054.
[30] A.M. Fourie, J.F. Sambrook, M.J. Gething, Common and divergent peptide binding specificities of hsp70 molecular chaperones, J. Biol. Chem. 269 (1994) 30470–30478.
[31] L. Shaner, R. Sousa, K.A. Morano, Characterization of Hsp70 binding and nucleotide exchange by the yeast Hsp110 chaperone Sse1, Biochemistry 45 (2006) 15075–15084.
[32] N. Yamagishi, K. Ishihara, T. Hatayama, Hsp105alpha suppresses Hsc70 chaperone activity by inhibiting Hsc70 ATPase activity, J. Biol. Chem. 279 (2004) 41727–41733.
[33] L. Packschies, H. Theyssen, A. Buchberger, B. Bukau, R.S. Goody, J. Reinstein, GrpE accelerates nucleotide exchange of the molecular chaperone DnaK with an associative displacement mechanism, Biochemistry 36 (1997) 3417–3422.
[34] G. Celaya, J.A. Fernandez-Higuero, I. Martin, G. Rivas, F. Moro, A. Muga, Crowding modulates the conformation, affinity, and activity of the components of the bacterial disaggregase machinery, J. Mol. Biol. 428 (2016) 2474–2487.
[35] T. Laufen, M.P. Mayer, C. Beisel, D. Klostermeier, A. Mogk, J. Reinstein, et al., Mechanism of regulation of hsp70 chaperones by DnaJ cochaperones, Proc. Natl. Acad. Sci. U. S. A. 96 (1999) 5452–5457.
[36] H. Raviol, H. Sadlish, F. Rodriguez, M.P. Mayer, B. Bukau, Chaperone network in the yeast cytosol: Hsp110 is revealed as an Hsp70 nucleotide exchange factor, EMBO J. 25 (2006) 2510–2518.
[37] D. Brehmer, C. Gassler, W. Rist, M.P. Mayer, B. Bukau, Influence of GrpE on DnaK–substrate interactions, J. Biol. Chem. 279 (2004) 27957–27964.
[38] F. Moro, S.G. Taneva, A. Velazquez-Campoy, A. Muga, GrpE N-terminal domain contributes to the interaction with Dnak and modulates the dynamics of the chaperone substrate binding domain, J. Mol. Biol. 374 (2007) 1054–1064.
[39] M.P. Mayer, H. Schroder, S. Rudiger, K. Paal, T. Laufen, B. Bukau, Multistep mechanism of substrate binding determines chaperone activity of Hsp70, Nat. Struct. Biol. 7 (2000) 586–593.
[40] S. Diamant, P. Goloubinoff, Temperature-controlled activity of DnaK–DnaJ–GrpE chaperones: protein-folding arrest and recovery during and after heat shock depends on the substrate protein and the GrpE concentration, Biochemistry 37 (1998) 9688–9694.
[41] S. Sugimoto, K. Saruwatari, C. Higashi, K. Sonomoto, The proper ratio of GrpE to DnaK is important for protein quality control by the DnaK–DnaJ–GrpE chaperone system and for cell division, Microbiology 154 (2008) 1876–1885.
[42] A. Finka, S.K. Sharma, P. Goloubinoff, Multi-layered molecular mechanisms of polypeptide holding, unfolding and disaggregation by HSP70/HSP110 chaperones, Front. Mol. Biosci. 2 (2015) 29.
[43] S.P. Acebron, V. Fernandez-Saiz, S.G. Taneva, F. Moro, A. Muga, DnaJ recruits DnaK to protein aggregates, J. Biol. Chem. 283 (2008) 1381–1390.
[44] J. Winkler, J. Tyedmers, B. Bukau, A. Mogk, Hsp70 targets Hsp100 chaperones to substrates for protein disaggregation and prion fragmentation, J. Cell Biol. 198 (2012) 387–404.
[45] C. Schlieker, J. Weibezahn, H. Patzelt, P. Tessarz, C. Strub, K. Zeth, et al., Substrate recognition by the AAA+ chaperone ClpB, Nat. Struct. Mol. Biol. 11 (2004) 607–615.
[46] X. Xu, E.B. Sarbeng, C. Vorvis, D.P. Kumar, L. Zhou, Q. Liu, Unique peptide substrate binding properties of 110-kDa heat-shock protein (Hsp110) determine its distinct chaperone activity, J. Biol. Chem. 287 (2012) 5661–5672.
[47] J. Hohfeld, S. Jentsch, GrpE-like regulation of the hsc70 chaperone by the anti-apoptotic protein BAG-1, EMBO J. 16 (1997) 6209–6216.
[48] C.S. Gassler, T. Wiederkehr, D. Brehmer, B. Bukau, M.P. Mayer, Bag-1M accelerates nucleotide release for human Hsc70 and Hsp70 and can act concentration-dependent as positive and negative cofactor, J. Biol. Chem. 276 (2001) 32538–32544.
[49] J.N. Rauch, J.E. Gestwicki, Binding of human nucleotide exchange factors to heat shock protein 70 (Hsp70) generates functionally distinct complexes in vitro, J. Biol. Chem. 289 (2014) 1402–1414.
[50] N. Yamagishi, H. Nishihori, K. Ishihara, K. Ohtsuka, T. Hatayama, Modulation of the chaperone activities of Hsc70/Hsp40 by Hsp105alpha and Hsp105beta, Biochem. Biophys. Res. Commun. 272 (2000) 850–855.
[51] J.P. Grimshaw, I. Jelesarov, H.J. Schonfeld, P. Christen, Reversible thermal transition in GrpE, the nucleotide exchange factor of the DnaK heat-shock system, J. Biol. Chem. 276 (2001) 6098–6104.
[52] F. Moro, A. Muga, Thermal adaptation of the yeast mitochondrial Hsp70 system is regulated by the reversible

unfolding of its nucleotide exchange factor, J. Mol. Biol. 358 (2006) 1367–1377.
[53] R. Melero, F. Moro, M.A. Perez-Calvo, J. Perales-Calvo, L. Quintana-Gallardo, O. Llorca, et al., Modulation of the chaperone DnaK allosterism by the nucleotide exchange factor GrpE, J. Biol. Chem. 290 (2015) 10083–10092.
[54] C. Andreasson, J. Fiaux, H. Rampelt, S. Druffel-Augustin, B. Bukau, Insights into the structural dynamics of the Hsp110–Hsp70 interaction reveal the mechanism for nucleotide exchange activity, Proc. Natl. Acad. Sci. U. S. A. 105 (2008) 16519–16524.
[55] J.L. Goeckeler, A.P. Petruso, J. Aguirre, C.C. Clement, G. Chiosis, J.L. Brodsky, The yeast Hsp110, Sse1p, exhibits high-affinity peptide binding, FEBS Lett. 582 (2008) 2393–2396.
[56] P.V. Konarev, V.V. Volkov, A.V. Sokolova, M.H.J. Koch, D.I. Svergun, PRIMUS—a Windows-PC based system for small-angle scattering data analysis, J. Appl. Crystallogr. 36 (2003) 1277–1282.
[57] A. Guinier, La diffraction des rayon's X aux tres petits angles: application a l'etude de phenomenes ultramicroscopies, Ann. Phys. 12 (1939) 161–237.
[58] D.I. Svergun, Determination of the regularization parameter in indirect-transform methods using perceptual criteria, J. Appl. Crystallogr. 25 (1939) 495–503.
[59] R.P. Rambo, J.A. Tainer, Accurate assessment of mass, models and resolution by small-angle scattering, Nature 496 (2013) 477–481.
[60] D. Franke, D.I. Svergun, DAMMIF, a program for rapid ab-initio shape determination in small-angle scattering, J. Appl. Crystallogr. 42 (2009) 342–346.
[61] D.I. Svergun, Restoring low resolution structure of biological macromolecules from solution scattering using simulated annealing, Biophys. J. 76 (1999) 2879–2886.
[62] M.V. Petoukhov, D. Franke, A.V. Shkumatov, G. Tria, A.G. Kikhney, M. Gajda, C. Gorba, H.D.T. Mertens, P.V. Konarev, D.I. Svergun, New developments in the ATSAS program package for small-angle scattering data analysis, J. Appl. Crystallogr. 45 (2012) 342–350.
[63] L.A. Kelley, S. Mezulis, C.M. Yates, M.N. Wass, M.J. Stenberg, The Phyre2 web portal for protein modeling, prediction and analysis, Nat. Protoc. 10 (2015) 845–858.
[64] A. Lamiable, P. Thévenet, J. Rey, M. Vavrusa, P. Derreumaux, P. Tufféry, PEP-FOLD3: faster de novo structure prediction for linear peptides in solution and in complex, Nucleic Acids Res. 44 (W1) (2016) W449–W454.
[65] A. Panjkovich, D.I. Svergun, Deciphering conformational transitions of proteins by small angle X-ray scattering and normal mode analysis, Phys. Chem. Chem. Phys. 18 (2016) 5707–5719.
[66] S. Diamant, A.P. Ben-Zvi, B. Bukau, P. Goloubinoff, Size-dependent disaggregation of stable protein aggregates by the DnaK chaperone machinery, J. Biol. Chem. 275 (2000) 21107–21113.
[67] I. Martin, G. Celaya, C. Alfonso, F. Moro, G. Rivas, A. Muga, Crowding activates ClpB and enhances its association with DnaK for efficient protein aggregate reactivation, Biophys. J. 106 (2014) 2017–2027.
[68] J.G. Norby, Coupled assay of Na+,K+-ATPase activity, Methods Enzymol. 156 (1988) 116–119.
[69] M. Horst, W. Oppliger, B. Feifel, G. Schatz, B.S. Glick, The mitochondrial protein import motor: dissociation of mitochondrial hsp70 from its membrane anchor requires ATP binding rather than ATP hydrolysis, Protein Sci. 5 (1996) 759–767.